Published in final edited form as:
JACC Cardiovasc Imaging. 2011 December ; 4(12): 1265–1273. doi:10.1016/j.jcmg.2011.04.024.

Cardiac MRI of Edema in Acute Myocardial Infarction using Cine Balanced SSFP: A Translational Study

Andreas Kumar, MD MSc[1], **Nirat Beohar, MD**[3], **Jain Mangalathu Arumana, Dipl Ing**[4], **Eric Larose, MD**[1], **Debiao Li, PhD**[4,5], **Matthias G Friedrich, MD**[2], and **Rohan Dharmakumar, PhD**[4,5,*]

[1]2725 Chemin Ste-Foy, Québec Heart and Lung Institute, Laval University, Québec City, Canada G1V 4G5

[2]1403 - 29th St, Foothills Hospital, SSB Suite 0700, Stephenson CMR Centre, Dept of Cardiac Sciences, University of Calgary, Calgary AB Canada T2N 2T9

[3]675 N. St. Clair, Galter 19-100, Dept of Cardiology, Northwestern University, Chicago IL USA 60601

[4]737 N Michigan Ave, Suite 1600, Dept of Radiology, Northwestern University, Chicago IL USA 60601

[5]8700 Beverly Blvd, Suite G-149D, Biomedical Imaging Research Institute, Dept of Biomedical Sciences, Cedars-Sinai Medical Center, Los Angeles CA USA 90048

Abstract

Objective—To investigate the capabilities of balanced steady-state-free-precession (bSSFP) MRI as a novel cine imaging approach for characterizing myocardial edema in animals and patients following reperfused myocardial infarction.

Background—Current MRI methods require two separate scans for assessment of myocardial edema and cardiac function.

Methods—Mini-pigs (n=13) with experimentally induced reperfused myocardial infarction and patients with reperfused STEMI (n=26) underwent MR scans on days 2–4 post reperfusion. Cine bSSFP, T2-STIR, and late-gadolinium enhancement (LGE) were performed at 1.5T. Cine bSSFP and T2-STIR images were acquired with body coil to mitigate surface coil bias. Signal, contrast and the area of edema were compared. Additional patients (n=10) were analyzed for the effect of

*Correspondence to: Rohan Dharmakumar, PhD, Director, Translational Cardiac Imaging Research, Biomedical Imaging Research Institute, Dept of Biomedical Sciences, Cedars-Sinai Medical Center, 8700 Beverly Blvd, Suite G-149D, Los Angeles, USA 90048, Phone: (310) 423-7641, rohandkumar@csmc.edu.

DISCLOSURES:

Dr. Rohan Dharmakumar and Dr. Debiao Li hold research grants from the National Institutes of Health/ the National Heart, Lung and Blood Institute. Both receive research support from Siemens Healthcare. Dr. Dharmakumar also holds a research grant from the American Heart Association.

Dr. Matthias G. Friedrich holds research grants from The Canadian Institutes of Health Research, the Canadian Diabetes Association, the Alberta Heritage Foundation for Medical Research, and the Heart and Stroke Foundation of Canada. He receives research support from Husky Energy, Pfizer Canada and Siemens Canada. He is a shareholder and scientific advisor for Circle Cardiovascular Imaging. Dr. Andreas Kumar holds a research grant from the Canadian Institutes of Health Research. He receives financial support for investigator-initiated research by Pfizer Canada. He is a medical advisor for Nordic Biotech, Switzerland.

microvascular obstruction on bSSFP. A receiver-operator-characteristic analysis was performed to assess the accuracy of edema detection.

Results—An area of hyperintense bSSFP signal consistent with edema was observed in the infarction zone (contrast-to-noise ratio (CNR) 37±13) in all animals and correlated well with the area of LGE (R=0.83, p<0.01). In all patients, T2-STIR and bSSFP images showed regional hyperintensity in the infarction zone. Normalized CNR were not different between T2-STIR and bSSFP. On a slice-basis, the volumes of hyperintensity on T2-STIR and bSSFP images correlated well (R=0.86, p<0.001), and their means were not different. When compared with T2-STIR, bSSFP was positive for edema in 25/26 patients (sensitivity of 96%) and was negative in all controls (specificity 100%). All patients with MVO showed a significant reduction of signal in the subendocardial infarction zone, compared to infarcted epicardial tissue without MVO (p<0.05).

Conclusion—Myocardial edema from STEMI can be detected using cine bSSFP imaging with image contrast similar to T2-STIR. This new imaging approach allows for evaluating cardiac function and edema simultaneously, thereby reducing patient scan time and increasing efficiency. Further work is necessary to optimize edema contrast in bSSFP images.

Keywords

STEMI; Edema; Infarction; CMR; cardiac phase-resolved

INTRODUCTION

T2-weighted cardiovascular magnetic resonance (CMR) has been successfully employed for discriminating between acute and chronic myocardial infarction, based on elevations in myocardial T2 due to tissue edema accompanying acute, but not chronic, myocardial infarction.(1) Furthermore, T2-weighted assessment of myocardial edema may allow for detection of acute coronary syndromes (2, 3), as well as the assessment of the area-at-risk and myocardial salvage.(4)

Currently, T2-weighted CMR is performed using fast spin-echo sequences, with double or triple inversion preparation to suppress signal from intracavity blood and/or fat,(1) or with a T2-preparation with balanced steady-state free precession (bSSFP) readouts.(5) Covering the entire left ventricle with T2-weighted CMR takes 8–15 minutes of time, which is undesirable in the setting of a possible acute coronary syndrome or acute myocardial infarction. Since these acquisitions are limited to a single cardiac phase, additional multi-phase (cine) scans are required to evaluate cardiac function, which significantly extends the duration of the clinical exams.

An alternate approach for ascertaining the presence of myocardial edema may be available through bSSFP imaging. Cine bSSFP imaging is a clinically established CMR method for the assessment of left and right ventricular volumes and function. It is known that bSSFP signals are influenced by T1, T2 (6), and magnetization transfer effects (7). With increased free water resulting from edema, T1 and T2 are both increased (8) and magnetization transfer is reduced (9). Although T2 and T1 effects are antagonistic in the setting of bSSFP imaging and will work to reduce the overall effect from relaxation changes, the residual relaxational contribution combined with alterations in magnetization transfer (10), it may be possible to visualize reperfused acute myocardial infarct territories as hyperintense zones relative to healthy/remote myocardium. Employing bSSFP imaging for the detection of edema in the setting of reperfused acute myocardial infarction would have important implications: (1) increased efficiency of cardiac exams; and (2) co-registration of cardiac function and tissue characterization for clinical use.

The aim of this study was to investigate whether bSSFP imaging can be used to visualize the presence of edema in acute myocardial infarction in a controlled swine model as well as in patients with acute reperfused ST-elevation myocardial infarction (STEMI), using a control group of healthy volunteers. We hypothesized that: (1) in animals and patients with reperfused acute myocardial infarction, bSSFP will yield a hyperintense signal in the infarction zone as compared to the remote zone; (2) in healthy volunteers, bSSFP signals are homogenous throughout the myocardium in the absence of edema as determined by T2-STIR imaging.

METHODS

Animal Studies

The animal study protocol was reviewed and approved by the Institutional Animals Care and Usage Committee.

Animal Preparation—In 15 Yucatan mini-pigs (body weight 25–30 kg), myocardial infarction was induced as follows: The animals were anesthetized and mechanically ventilated with isoflurane. The right femoral artery was cannulated, and a guide catheter was advanced into the left circumflex artery. A balloon catheter was positioned in the proximal third of the artery and inflated to achieve complete occlusion of the artery. Success of coronary artery occlusion was controlled angiographically and by EKG recording of ST-elevation. The occlusion was released after 90 minutes and animals were allowed to recover for 2–3 days.

Prior to CMR imaging, each mini-pig was sedated, intubated, and placed on a ventilator and systemic O_2 saturation, end-tidal P_{CO2}, and heart rate were continuously monitored.

Imaging Protocol—All animal studies were performed on a clinical 1.5T MRI system (Sonata®, Siemens, Erlangen, Germany). Animals were positioned in a feet-first right-anterior oblique position and a flexible, phased-array surface coil, was placed over the chest. Scout images were obtained to localize the true axes of heart and whole-heart shimming was performed. Subsequently, multiple contiguous short-axis 2D bSSFP images were acquired in the cine mode covering the whole left ventricle (LV), using a standard cine bSSFP sequence (scan parameters: voxel size=0.9×0.9×6 mm^3; flip-angle=65°; T_R/T_E=3.1/1.5ms; readout bandwidth=930 Hz/pixel; 25 cardiac phases) with 2–3 signal averages. Subsequently, a gadolinium-based contrast agent was injected intravenously (Gd-DTPA, Magnevist®, Berlex Laboratories Inc., New Jersey, USA) at a dose of 0.1 mmol/kg and late gadolinium enhancement (LGE) imaging was performed 10–15 minutes post contrast injection. LGE acquisitions were breath-held, triggered to end systole, and covered the entire LV with the same slice positions used for cine bSSFP imaging. LGE images were acquired in end systole to have the largest myocardial surface for analysis while minimizing cardiac motion. LGE-CMR images were acquired using an inversion-recovery turbo FLASH sequence with the following scan parameters: T_R of 1 R-R interval; T_E=1.1; T_I=200–240 ms; flip-angle=25°; voxel size=1.3 ×1.3×6 mm^3; and same field-of-view as bSSFP scans.

Human Studies

The study protocol for volunteers and patients was reviewed and approved by the Institutional Ethics Committee, and written informed consent was obtained from every participant.

Imaging Protocol—All studies in humans were performed on a clinical 1.5T MRI system (Avanto®, Siemens Medical Solutions, Erlangen, Germany). The anatomical axes of the

heart were determined and a whole-heart shim was performed. In healthy volunteers (n =8, age 30±8 years, 4 females, no evidence of heart disease), a short-axis slice was obtained at a mid-ventricular level, using a cine bSSFP sequence followed by a T2-STIR sequence. In patients (n=27 without MVO as defined by LGE, and n=10 with MVO, all enrolled within 4 days after successful angioplasty for a first STEMI, as defined by American Heart Association diagnostic criteria), the sequences were prescribed along the mid-ventricular short-axis slice. LGE-CMR was performed with the same Gd-DTPA dose and imaging sequence. Typical imaging parameters for bSSFP were: field-of-view=340mm × 276mm; imaging matrix=192×156; slice thickness=10mm; flip-angle = 65°; T_R/T_E=3.32/1.16ms; bandwidth = 930 Hz/pixel; and 25 cardiac phases. Typical imaging parameters for T2-STIR imaging were: field-of-view=380mm × 309 mm; matrix=256×208; slice thickness=10mm; mid-diastolic acquisition; echo-train-length=25; T_R=2 heart beats; T_E=61ms; and bandwidth=245 Hz/pixel. Both bSSFP and T2-STIR images were acquired with the body coil. Typical LGE-CMR imaging parameters were: T_R=1 R-R interval; T_E=3.32ms; bandwidth=235 Hz/pixel; field-of-view=400mm × 300mm; imaging matrix=256×192; slice thickness=10mm. No image-acceleration methods were employed in this study.

Image analysis - Animals

CMR analysis was performed to test for infarction-dependent signal differences on bSSFP as follows: based on trigger times, LGE-CMR and cine bSSFP images were matched. Image analysis was performed using Matlab 7.0® (The MathWorks, Natick, Massachusetts, USA). On the basis of LGE-CMR images, remote (non-infarcted) regions of the myocardium were identified, and the mean (S_r) and standard deviation (SD) of the signal intensities of these regions were computed in the LGE and bSSFP images. Similar to previous studies (1, 2), pixels with signal intensities > 2SD of the remote areas of the bSSFP images were identified as regions of edema and were used to compute the mean signal within the hyperintense zones (S) and total area of edema. The infarct zone was identified as the myocardial region with signal intensities > 5SD of the mean signal intensity from the remote regions, as described previously (11). Using this criterion, the infarct zones were identified on a pixel-by-pixel basis and the total infarct areas and the corresponding average signal intensities of the infarct areas were computed. This was performed on every imaging slice positive for LGE-CMR. From the measured bSSFP signal intensities, average signal-to-noise ratios (SNR) of infarction zones were computed for each animal, using SNR= $S/\lceil$, where $\lceil$ was the standard deviation of noise (air). Contrast-to-noise ratios (CNR) were computed using CNR=$(S - S_r)/\lceil$.

Image analysis- Healthy Volunteers

In healthy volunteers, myocardial signal homogeneity was assessed on bSSFP and T2-STIR images, using a validated software (cmr$^{42®}$, Circle Cardiovascular Imaging Inc., Calgary Canada), to rule out false positive signal as follows: Representative regions of interest (ROI) were drawn manually on the T2-STIR images in the anterior wall, septum, inferior wall and lateral wall, and copied to the corresponding frame of the cine bSSFP. Signal intensities were measured for these ROIs. SNR was computed in a manner similar to earlier. To assess signal homogeneity throughout the myocardium, the SNR of ROIs in the anterior, septal, inferior and lateral walls were compared.

Image Analysis- Patients

To assess for myocardial edema, T2-STIR and bSSFP images of patients with acute reperfused myocardial infarction were analyzed, using cmr$^{42®}$, as follows: based on trigger times, T2-STIR and cine bSSFP images were matched. On T2-STIR images, a ROI was drawn in remote myocardium not affected by the infarct. Using the threshold-based signal detection, as described above (animal studies), remote and edematous territories were

identified (Figure 1). The signal intensity of the remote and the area and signal intensity of edematous myocardium were measured. The ROIs were then copied to the bSSFP images, and signal measurements repeated. In general, contrast was calculated as [(Mean SI (infarct) − Mean SI (remote) / Mean SI (remote)] × 100%, where SI denotes signal intensity. For MVO, contrast was calculated as [(Mean SI (infarct zone without MVO) − Mean SI (MVO)] / Mean SI (infarct zone without MVO). MVOs were identified as hypointense regions in LGE images. bSSFP signal intensity from the MVOs were measured by manually drawing the ROIs in hypointense cores of LGE images and copying onto the corresponding frame of bSSFP cine images. Contrast-to-noise ratio (CNR) was computed as [(Mean SI (infarct) − Mean SI (remote) / SD of noise]. To account for the differences in acquisition bandwidth and spatial resolution between T2-STIR and bSSFP images, normalized CNR (adjusting for voxel volume and imaging BW), defined as $CNR_{norm}=SNR_{norm}$ (infarct) − SNR_{norm} (remote) was calculated, where $SNR_{norm}=SNR \times (BW)^{1/2}$/voxel volume, and BW is bandwidth. Subsequently, threshold-based signal detection was performed on bSSFP and LGE images, as described above.

Statistics

Signal and contrast values were compared using a paired t-test for two variables, and using one-way ANOVA for multiple variables. Pearson correlation statistics were used to compare signal measurements and areas of pathology. The difference in the threshold-based measurement of area of edema using T2-STIR and bSSFP was measured as an absolute and % difference, and a Bland-Altman Plot was created. No correction was made for multiple correlated observations within individuals. Receiver-operator-characteristic analysis, taking T2-STIR images to provide the ground truth, was performed using image contrast values computed from regional SI measurements obtained from patients and from healthy volunteers. Image contrast in bSSFP images from volunteers were computed as relative percent signal differences by arbitrarily assigning one of the walls to be edematous and another to be remote. More specifically, contrast values were computed between lateral and septal, anterior and septal, inferior and septal, lateral and anterior, and anterior and inferior walls. In total, 66 contrast values were obtained and utilized to derive the receiver-operator-characteristic curves (26 data points from patients positive for edema, and 40 data points from volunteers not-positive for edema). StatPlus:mac® Version 5.2.0 (AnalystSoft Inc., Alexandria, Virginia, USA), and SPSS16® for Mac, (SPSS Inc. Chicago, Illinois, USA), Microcal Origin 7.0 (OriginLab Corp, Northampton, Massachusetts, USA) were used for data analysis. Values are given as mean ± standard deviation. Results were deemed significant for $p<0.05$.

RESULTS

Animal Studies

Two out of the 15 mini-pigs succumbed to fatal ventricular arrhythmia. A total of 13 pigs completed the protocol with and were available for analysis. Based on LGE-CMR images obtained over the whole LV in each animal, 2 to 4 short-axis slices per pig were observed to have hyperintense myocardial territories consistent with acute myocardial infarction.

A set of typical short-axis cine bSSFP images obtained from the mid-ventricle of a mini-pig and the corresponding LGE-CMR image (at end-systole) are shown in Figure 2. The hyperintense areas, computed on the basis of threshold-based detection performed on bSSFP and LGE images, were highly correlated (Pearson R=0.83, $p< 0.01$, see Figure 3), with the line of best fit given by $A_{SSFP} = 1.07A_{LGE} + 0.41$, where A_{SSFP} and A_{LGE} denote the hyperintense myocardial area (cm^2) measured from the bSSFP and LGE images, respectively. The SNR of the infarction zones on bSSFP images were significantly higher

than that of the remote myocardium (bSSFP SNR: 85.9±8.4 (infarct) vs 59.4±7.2 (remote)), resulting in CNR of 37.2±12.6. Mean SNR values between healthy (59.4) and affected regions (85.9) with a pooled standard deviation of 15.6 were significantly different ($p<0.0001$).

Healthy Volunteers

In healthy volunteers, the signal measured in the anterior, septal, inferior and lateral walls of the myocardium was homogeneous (SI anterior 162±12, SI septum 165±4, SI inferior 160±10, SI lateral 151±14; ANOVA $p=0.08$).

Patients

From the 27 patients without MVO, one patient was excluded because of absence of CMR findings consistent with acute myocardial infarction, despite a clinical diagnosis of STEMI. The remaining 26 patients (57±9 years, 4 female) used for analysis had infarcts in the anterior/septal territory (n=13), inferior territory (n=9), or lateral territory (n=4). Example images from different infarct locations are shown in Figure 4; phase-resolved images from a representative patient are shown in Figure 5. Ten patients with MVO were all male, age 58±9 years, and had myocardial infarction of the anterior-septal territory (n=5), inferior territory (n=4) or lateral territory (n=1).

On T2-STIR images, the SI in the infarct zone was higher than that in remote myocardium (SI: 373±107 (infarction) vs. 229±75 (remote), $p<0.001$). Likewise, on the corresponding bSSFP CMR (matched for cardiac phase), the SI in the infarcted myocardium was greater than that of remote myocardium (bSSFP SI: 253±41 (infracted) vs. 162±28 (remote), $p<0.001$). The infarction-to-remote myocardium contrast measured on T2-STIR was not different from the contrast measured on bSSFP (contrast T2-STIR 67±33 vs. bSSFP 59±26, $p=0.31$). Likewise, normalized CNR was also not different between T2-STIR and bSSFP (CNR_{norm}: 8.08±4.14 (T2-STIR) vs. 7.50±2.96 (bSSFP), $p=0.53$).

The mean infarction volume (single slice) on LGE-CMR was 4.1±1.4ml. Edema volumes on T2-STIR images correlated well with edema volumes measured on bSSFP images (Pearson $R=0.86$, $p<0.001$, Figure 6). The volume of edematous tissue (single slice) measured on T2-STIR correlated with infarct size (Pearson $R=0.54$, $p<0.01$); edematous tissue volumes on bSSFP also correlated with infarct size (Pearson $R=0.47$, $p=0.02$). The edema volume measured by T2-STIR were not significantly different from those measured with bSSFP (volume of edema on single slice: 6.0±2.3ml (T2-STIR) vs. 4.9±2.1ml (bSSFP), $p=0.07$). A Bland-Altman Plot displaying the difference between the measurements using both methods is shown in Figure 7.

Receiver-operator-characteristic analysis of bSSFP images obtained from patients and volunteers showed the following: (a) area-under-the-curve: 0.99; (b) sensitivity: 96%; and (c) specificity: 100%.

MVOs consistently yielded reduced signal intensity on bSSFP images compared to the infarction zone without MVO (mean signal intensity from infarcted regions with MVO was 262±27, and MVO zone was 197±33, $p<0.001$ for the difference). The contrast between MVO and non-MVO infarction territories was 25±8%. The mean signal intensity from MVO territories was still higher than from remote myocardium (MVO zone 197±33, remote myocardium 154±41, $p<0.05$ for the difference).

DISCUSSION

We demonstrated that cine bSSFP can detect edema-related signal in reperfused acute myocardial infarcts, in a swine model as well as in patients. In every animal and patient, bSSFP signal was higher in the acute myocardial infarct zone as compared to remote myocardium. Consistent with myocardial edema and the representation of the area-at-risk (4, 12), the zone of high signal on bSSFP was consistently larger than the zone of irreversible injury as assessed by LGE-CMR, in animals and patients. The volume of edema measured by bSSFP was not different from T2-STIR, on a slice-to-slice basis. Receiver-operator-characteristic analysis revealed that T2-STIR and bSSFP images have nearly the same sensitivity and specificity for identifying myocardial edema associated with STEMI. Zones of microvascular obstruction yielded a lower signal on bSSFP, compared to infarcted tissue without microvascular obstruction.

T2-weighted imaging plays a key role in the assessment of patients with myocardial infarction. Its ability to detect myocardial edema (2, 8) allows for the differentiation of acute from chronic myocardial injury (1), the measurement of the area-at-risk (4, 13), and the identification of the perfusion territory subject to ischemic injury. This facilitates in the diagnosis of the culprit coronary artery (1). In conjunction with LGE-CMR, T2-weighted-CMR allows for the assessment of myocardial salvage (12, 14). Commonly, T2-weighted fast spin-echo images, limited to a single cardiac phase, are clinically used to assess myocardial edema. The approach we presented here using bSSFP has important advantages over the most commonly utilized T2-weighted edema imaging methods, from a clinical as well as a research perspective.

Clinical perspective

Time is of essence when using CMR because of the high operating costs of scanners and required staff. Any approach that successfully reduces scanner time will lead to more cost-efficient protocols. Time-efficient imaging protocols benefit patients with acute heart disease such as myocardial infarction, because a delay of therapy in the acute phase is associated with an increase in mortality. While the benefits of T2-weighted CMR in patients suspected of suffering from a non-ST elevation acute coronary syndrome has been demonstrated (3), the prescription of the complete imaging protocol requires approximately 45 minutes of scan time, during which viable myocardium-at-risk may be lost to necrosis. Likewise, in hospitalized patients with acute reperfused STEMI, it is important to keep imaging times as short as possible because these patients are at risk for life-threatening arrhythmia and heart failure. In commonly used CMR protocols, approximately one third of that imaging time is dedicated to whole-heart T2-weighted imaging. Deriving equivalent information from bSSFP would provide opportunities to save nearly 15 minutes of valuable time by obtaining edema and function information (“two for one”). This may help increase patient throughput, decrease waiting time for CMR studies, and make CMR available for more patients.

Research perspective

While the role of edema in acute myocardial infarction is largely recognized, a number of questions regarding edema pathophysiology remain unsolved. The imaging approach we investigated here can be applied in a cine manner. This would lay the groundwork for further investigation into the effects of edema on infarction pathophysiology at a moderately high temporal resolution, and the investigation of edema at different phases of the cardiac cycle. Edema plays a role in a number of non-ischemic cardiomyopathies as well;(15–17) future investigations would have to establish the role of bSSFP imaging for edema in these settings.

Technical issues, Limitations

This is a pilot study with a limited sample size in animals and humans. Nevertheless, the results are consistent across the different analysis groups (healthy volunteers, and animals and patients with acute myocardial infarction). In healthy subjects and in patients, to remove potential coil bias, the body coil was used. This may lead to a reduction in SNR compared to what one would expect with a cardiac (surface) coil. However, by using the body coil, a uniform signal was achieved for all myocardial walls. We deemed a uniform signal with the body coil to be more important than optimal SNR with a cardiac coil. Nevertheless, even with the body coil applied here, the SNR was sufficient for clinical imaging. Technical improvements that lead to better coil bias corrections are expected to enable the use of cardiac surface coil for edema imaging with cine bSSFP. This will significantly increase the SNR and the ability to visualize edema without manual windowing in bSSFP images.

Shimming is critically important for the use of myocardial edema imaging with bSSFP; incorrect shims can significantly degrade image quality and assessment of edema. Moreover, as this study utilized conventional cine bSSFP imaging to identify myocardial edema, possibilities of pulse sequence modifications to optimize SNR and CNR for edema assessment with cine bSSFP imaging need to be investigated. Given the indifference between the CNR_{norm} of T2-STIR and bSSFP approaches, one method to increase the CNR of bSSFP acquisitions is to decrease the acquisition bandwidth. While this is likely to increase the TR, which may make bSSFP imaging to more sensitive to off-resonance effects, careful shimming and center frequency selection may help overcome these artifacts. Alternatively, image-averaging approaches may be used to increase CNR of bSSFP based edema imaging (18).

In this study, bSSFP, T2-STIR, and LGE images were acquired from only a single (midventricular) slice per patient. This prevented us from reporting true volumetric comparison of edema between T2-STIR and bSSFP for each patient.

The receiver-operator-characteristic analyses and the sensitivity and specificity measures may be inflated due to the combination of STEMI patients with healthy controls. A more detailed study in a larger population size is expected to necessary to more accurately estimate the sensitivity and specificity of bSSFP MRI for detecting myocardial edema in the setting of acute myocardial infarction.

Although the threshold based, semi-quantitative image analysis applied here readily detected edema-related hyperintense signals in the affected regions, the performance of a visual, non-quantitative image analysis was not assessed in this study. Manual adjustment of image display for window and contrast may be necessary for optimal visualization of the edema zone.

Acknowledgments

FUNDING SOURCES: This work was supported by grants from NIH/NHLBI (HL091989) and the American Heart Association (SDG 0735099N).

ABBREVIATIONS

b-SSFP	Balanced steady state free precession
CNR	Contrast-to-noise ratio
EKG	electrocardiogram

Gd-DTPA	Gadolinium-diethylene-triamine-pentaacetic acid
LGE	Late gadolinium enhancement
ROI	Region of interest
SD	Standard deviation
SI	Signal intensity
STEMI	ST-elevation myocardial infarction
T2-STIR	T2-weighted Short TI Inversion Recovery
$\mathbf{T_E}$	Echo time
$\mathbf{T_I}$	Inversion time
$\mathbf{T_R}$	Repetition time

REFERENCES

1. Abdel-Aty H, Zagrosek A, Schulz-Menger J, et al. Delayed enhancement and T2-weighted cardiovascular magnetic resonance imaging differentiate acute from chronic myocardial infarction. Circulation. 2004; 109:2411–2416. [PubMed: 15123531]
2. Abdel-Aty H, Cocker M, Meek C, Tyberg JV, Friedrich MG. Edema as a very early marker for acute myocardial ischemia: a cardiovascular magnetic resonance study. J Am Coll Cardiol. 2009; 53:1194–1201. [PubMed: 19341860]
3. Cury RC, Shash K, Nagurney JT, et al. Cardiac magnetic resonance with T2-weighted imaging improves detection of patients with acute coronary syndrome in the emergency department. Circulation. 2008; 118:837–844. [PubMed: 18678772]
4. Aletras AH, Tilak GS, Natanzon A, et al. Retrospective determination of the area at risk for reperfused acute myocardial infarction with T2-weighted cardiac magnetic resonance imaging: histopathological and displacement encoding with stimulated echoes (DENSE) functional validations. Circulation. 2006; 113:1865–1870. [PubMed: 16606793]
5. Kellman P, Aletras AH, Mancini C, McVeigh ER, Arai AE. T2-prepared SSFP improves diagnostic confidence in edema imaging in acute myocardial infarction compared to turbo spin echo. Magn Reson Med. 2007; 57:891–897. [PubMed: 17457880]
6. Haacke, EM.; Brown, RW.; Thompson, MR.; Venkatesan, R. Magentic Resonance Imaging: Physical principles and sequence design. John-Wiley & and Sons Inc; New-York: 1999. Chapter 18; p. 451-512.
7. Bieri O, Scheffler K. On the origin of apparent low tissue signals in balanced SSFP. Magn Reson Med. 2006; 56:1067–1074. [PubMed: 17036284]
8. Higgins CB, Herfkens R, Lipton MJ, et al. Nuclear magnetic resonance imaging of acute myocardial infarction in dogs: alterations in magnetic relaxation times. Am J Cardiol. 1983; 52:184–188. [PubMed: 6858909]
9. Haraldseth O, Jones RA, Schjøtt J, Rinck PA, Jynge P, Oksendal AN. Early detection of regional myocardial ischemia in ex vivo piglet hearts: MR imaging with magnetization transfer. J Magn Reson Imaging. 1994 Jul–Aug; 4(4):603–608. [PubMed: 7949688]
10. Weber OM, Speier P, Scheffler K, Bieri O. Assessment of magnetization transfer effects in myocardial tissue using balanced steady-state free precession (bSSFP) cine MRI. Magn Reson Med. 2009; 62:699–705. [PubMed: 19572387]
11. Bondarenko O, Beek AM, Hofman MB, et al. Standardizing the definition of hyperenhancement in the quantitative assessment of infarct size and myocardial viability using delayed contrast-enhanced CMR. J Cardiovasc Magn Reson. 2005; 7:481–485. [PubMed: 15881532]
12. Friedrich MG, Abdel-Aty H, Taylor A, Schulz-Menger J, Messroghli D, Dietz R. The salvaged area at risk in reperfused acute myocardial infarction as visualized by cardiovascular magnetic resonance. J Am Coll Cardiol. 2008; 51:1581–1587. [PubMed: 18420102]

13. Garcia-Dorado D, Oliveras J, Gili J, et al. Analysis of myocardial oedema by magnetic resonance imaging early after coronary artery occlusion with or without reperfusion. Cardiovasc Res. 1993; 27:1462–1469. [PubMed: 8297415]
14. Ibanez B, Prat-Gonzalez S, Speidl WS, et al. Early metoprolol administration before coronary reperfusion results in increased myocardial salvage: analysis of ischemic myocardium at risk using cardiac magnetic resonance. Circulation. 2007; 115:2909–2916. [PubMed: 17515460]
15. Friedrich MG, Sechtem U, Schulz-Menger J, et al. Cardiovascular magnetic resonance in myocarditis: A JACC White Paper. J Am Coll Cardiol. 2009; 53:1475–1487. [PubMed: 19389557]
16. Abdel-Aty H, Cocker M, Friedrich MG. Myocardial edema is a feature of Tako-Tsubo cardiomyopathy and is related to the severity of systolic dysfunction: insights from T2-weighted cardiovascular magnetic resonance. Int J Cardiol. 2009; 132:291–293. [PubMed: 18086501]
17. Melacini P, Corbetti F, Calore C, et al. Cardiovascular magnetic resonance signs of ischemia in hypertrophic cardiomyopathy. Int J Cardiol. 2008; 128:364–373. [PubMed: 17643520]
18. Kellman P, Larson AC, Hsu LY, et al. Motion-corrected free-breathing delayed enhancement imaging of myocardial infarction. Magn Reson Med. 2005; 53:194–200. [PubMed: 15690519]

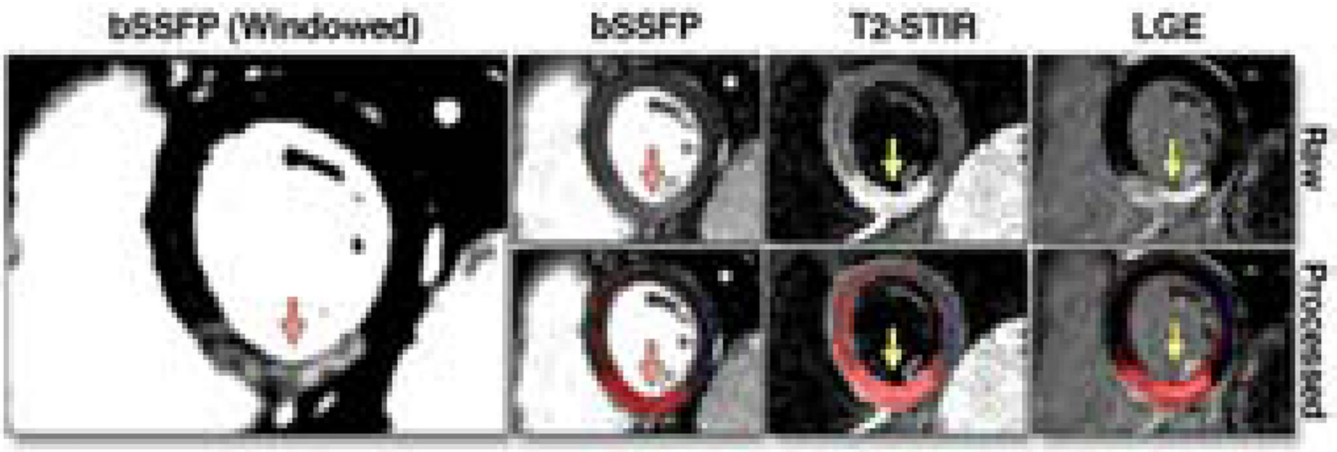

Figure 1. Representative image analysis in a 48-year-old male with first acute STEMI in the inferior territory

The larger image on the left is a windowed bSSFP image showing hyperintensity in the inferior wall. The upper panel shows the raw images. The lower panel shows the same images using semi-automatic threshold-based signal detection. Based on a reference region of interest in remote myocardium (here, the lateral wall), all pixels that have a signal intensity ≥ 2SD than the mean signal intensity of remote myocardium are automatically highlighted. This example also demonstrates that manual windowing may be necessary to better visualize edematous territories in bSSFP images with the naked eye.

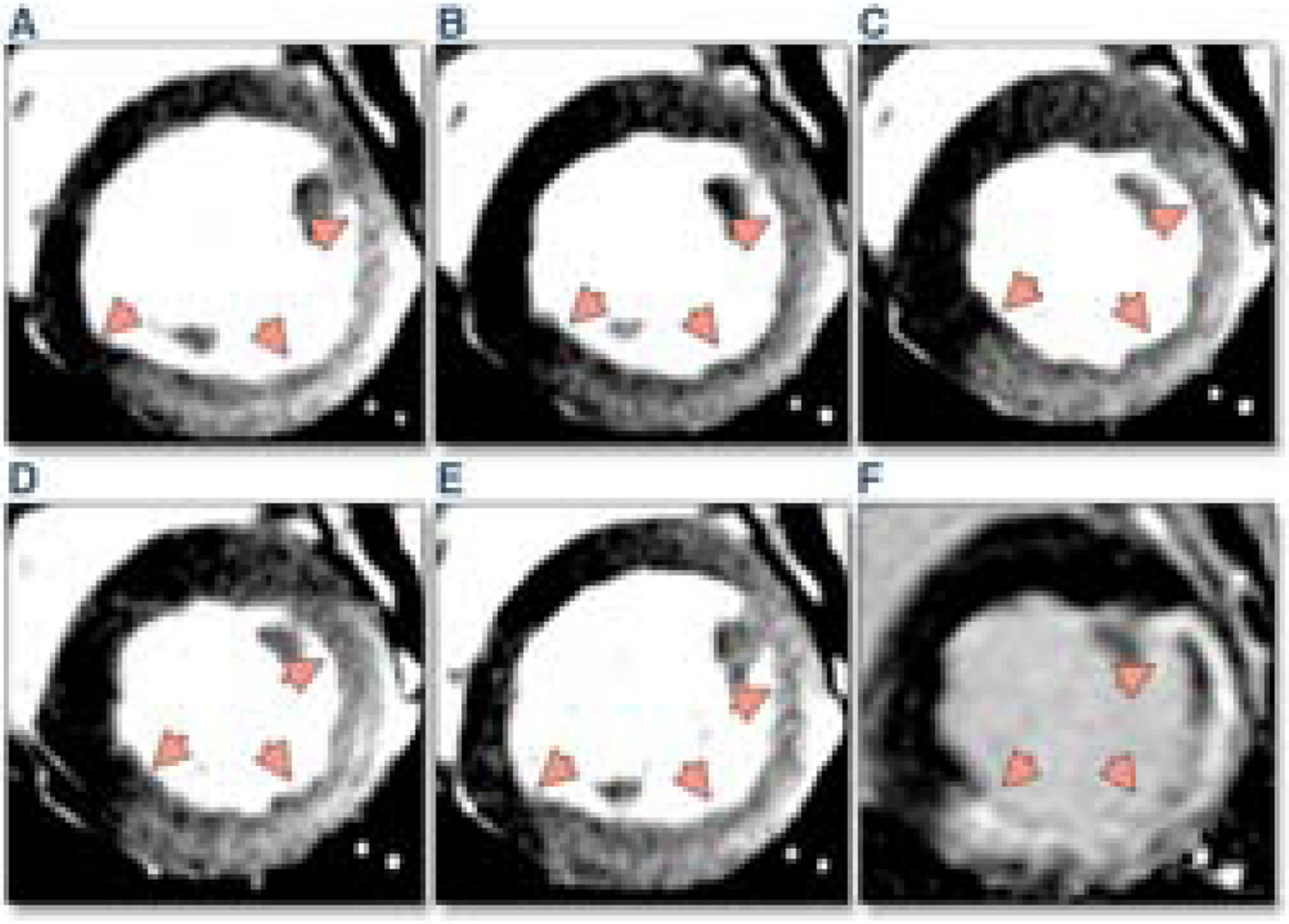

Figure 2. Cine bSSFP-based short axis magnetic resonance images (A–E) with the corresponding LGE image obtained at late systole (F) in an a swine that received a complete occlusion of the left circumflex artery for 90 min, followed by reperfusion

The set of cine images, acquired 3 days post infarction, clearly shows signal increase in the posterior wall, which is perfused by the left circumflex coronary artery. Also note the close correspondence between regional signal correspondence between bSSFP (A–E) and LGE (F) images. The trigger times (T_T) for the images: (A) T_T =0 ms; (B) T_T = 123 ms; (C) T_T = 245 ms; (D) T_T = 368 ms; (E) T_T =490 ms; (F) LGE T_T = 293 ms.

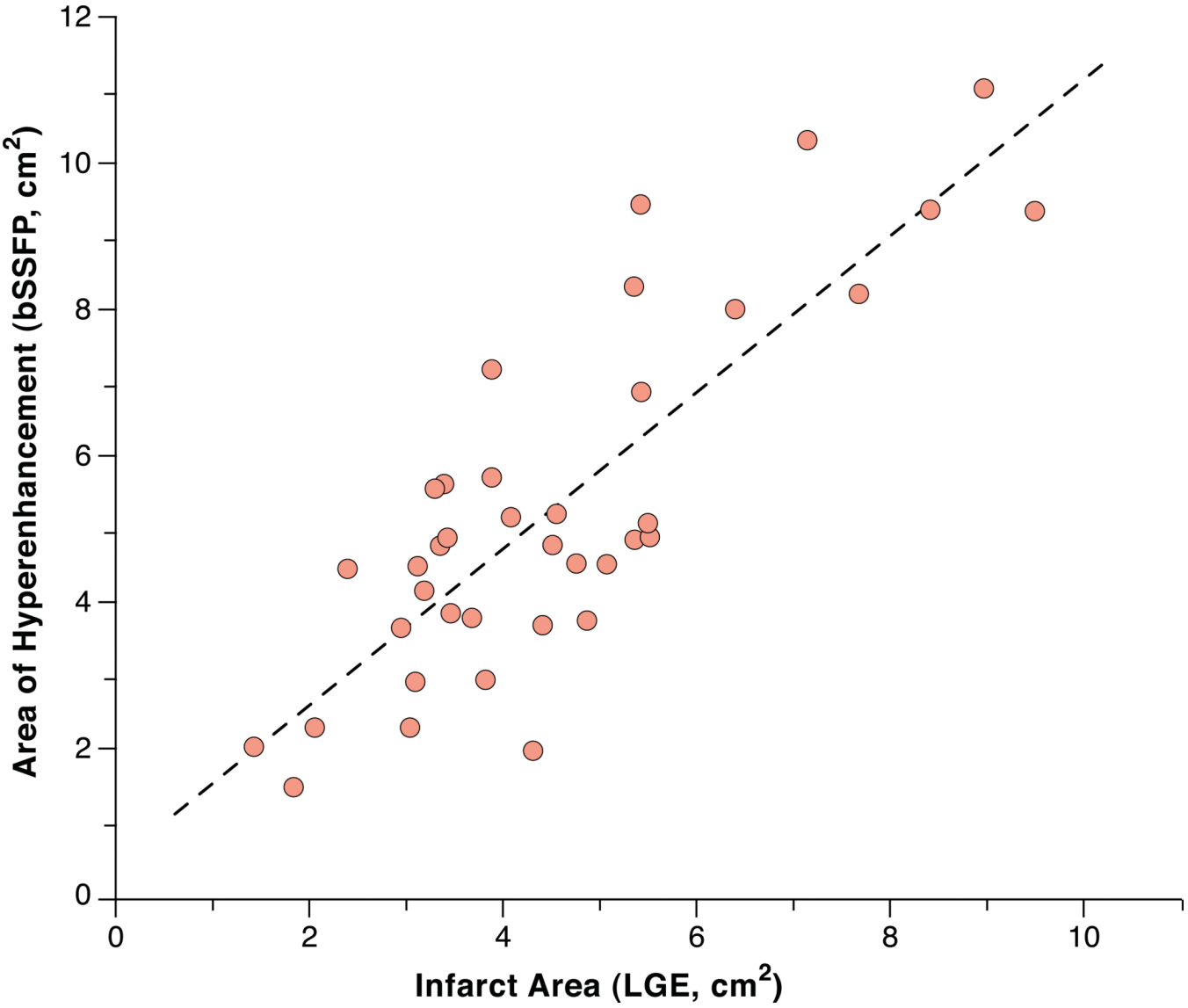

Figure 3. Scatter plot showing the correlation between infarct area computed from LGE (A_{LGE}) and area of edema computed from bSSFP (A_{SSFP}) images obtained from mini-pigs at late systole

The line of best fit is shown as a dashed line. Equation for line of best fit: $A_{SSFP} = 1.07 A_{LGE} + 0.41$. A strong correlation was observed between the two measures of infarct area ($R = 0.83$, $p<0.001$) with A_{SSFP} being larger than A_{LGE} (slope > 1).

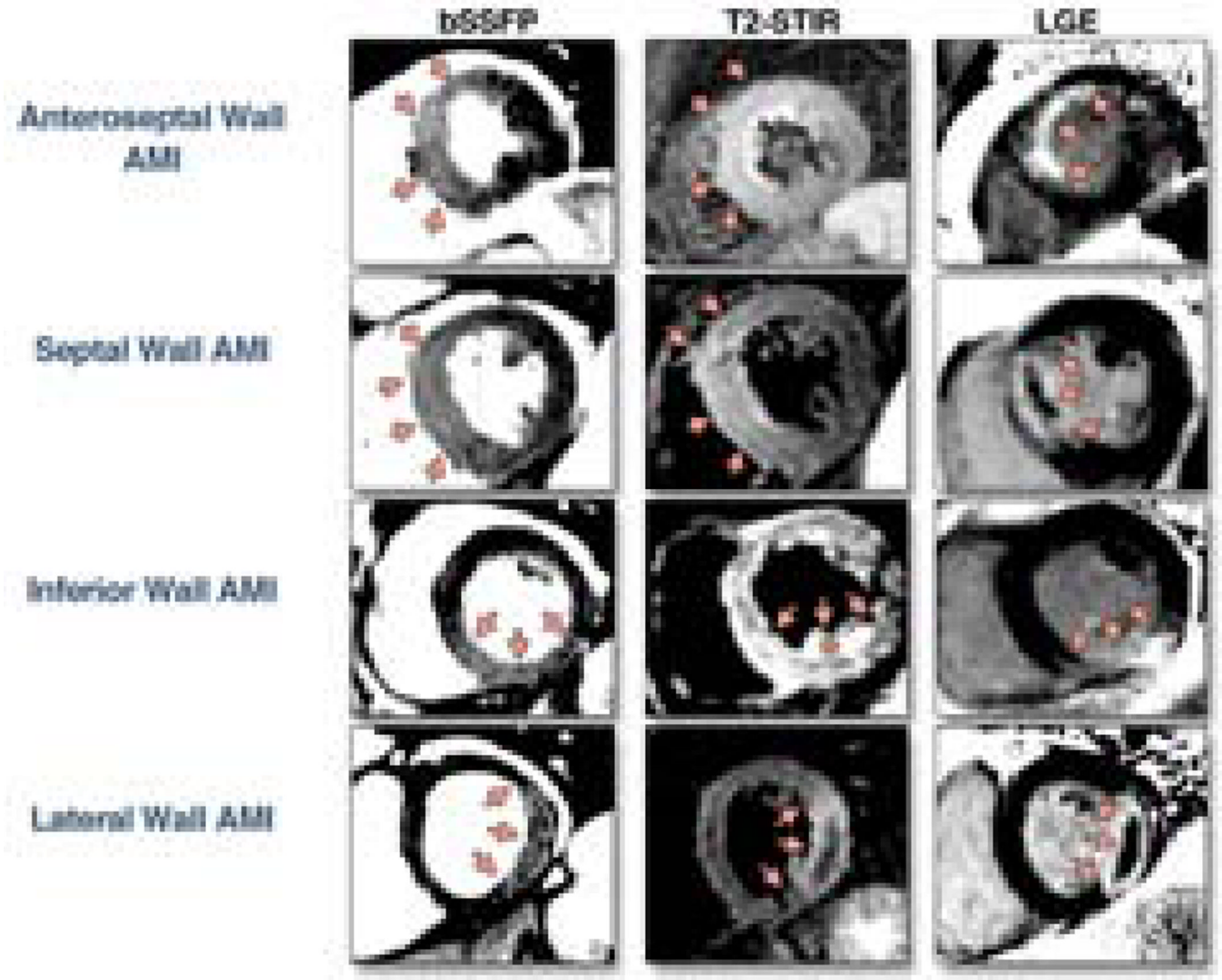

Figure 4. Example images from patients with reperfused ST-elevation myocardial infarction (STEMI)

Upper Panel: Anterior-septal STEMI in a 48 year old male. Upper middle panel: Septal STEMI in a 63 year old male. Lower middle panel: Inferior STEMI in a 61 year old male. Lower panel: Lateral wall STEMI in a 42 year old male. The bSSFP area of hyperintense signal (left column) corresponds well with the region of high signal on T2-STIR (middle column), but it exceeds the area of irreversible injury as imaged by LGE (right column). PSIR denotes phase-sensitive inversion recovery.

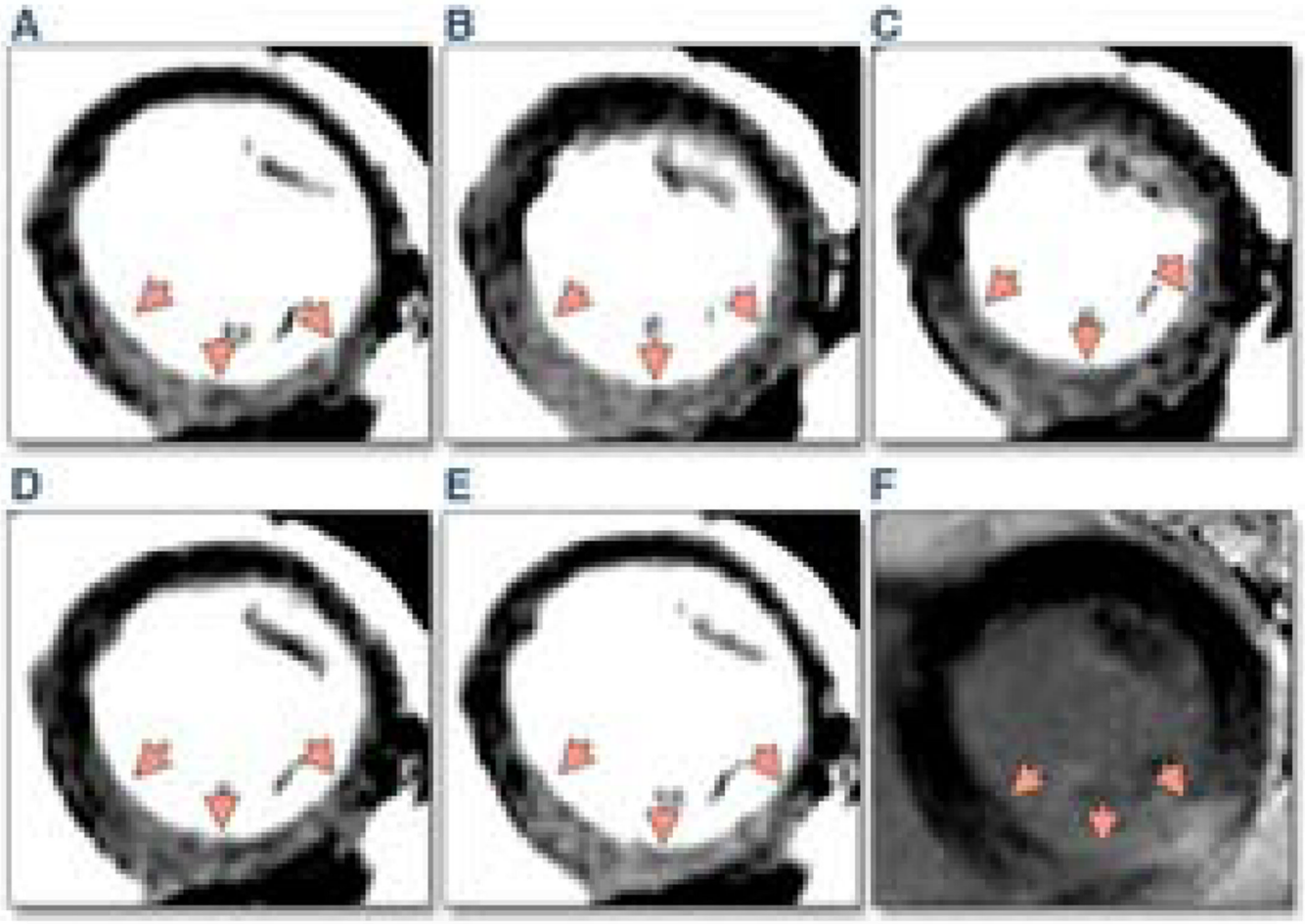

Figure 5. Cine bSSFP-based short-axis CMR images (A–E) with the corresponding LGE image obtained at late systole (F) from a patient with acute reperfused ST-elevation myocardial infarction in the territory of the right coronary artery

Note the close correspondence between signal increase patterns between the bSSFP (A–E) and LGE (F) images. The trigger times (T_T) for the images: (A) T_T =0 ms; (B) T_T = 198 ms; (C) T_T = 396 ms; (D) T_T = 594 ms; (E) T_T =792 ms; (F) LGE T_T = 455 ms.

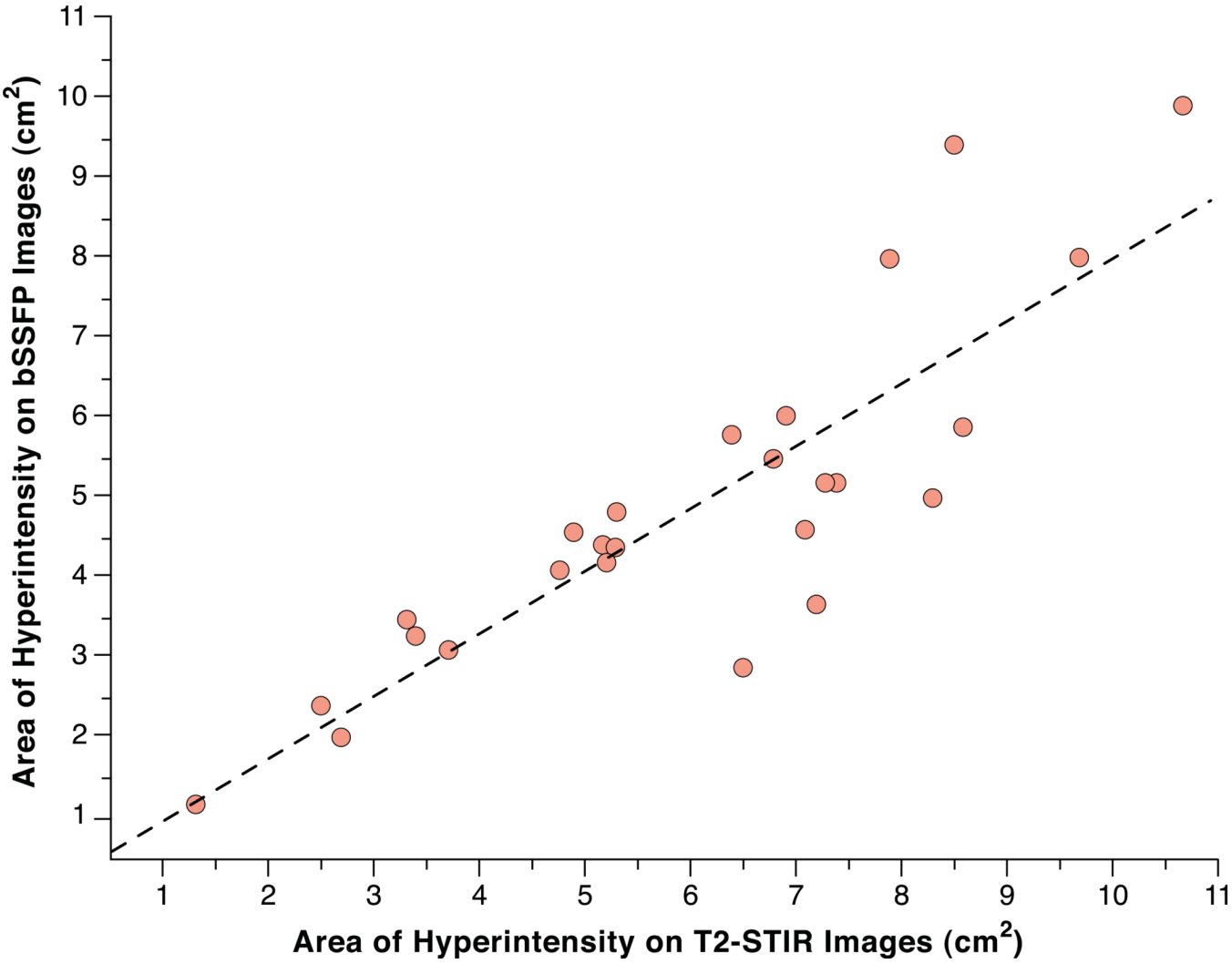

Figure 6. Scatter plot displaying the correlation between edematous areas (in patients) measured from T2-STIR and bSSFP with a semi-quantitative analysis

The line of best fit is shown as a dotted line. A strong correlation was observed between the two measures of edematous areas ($R = 0.86$, $p<0.001$).

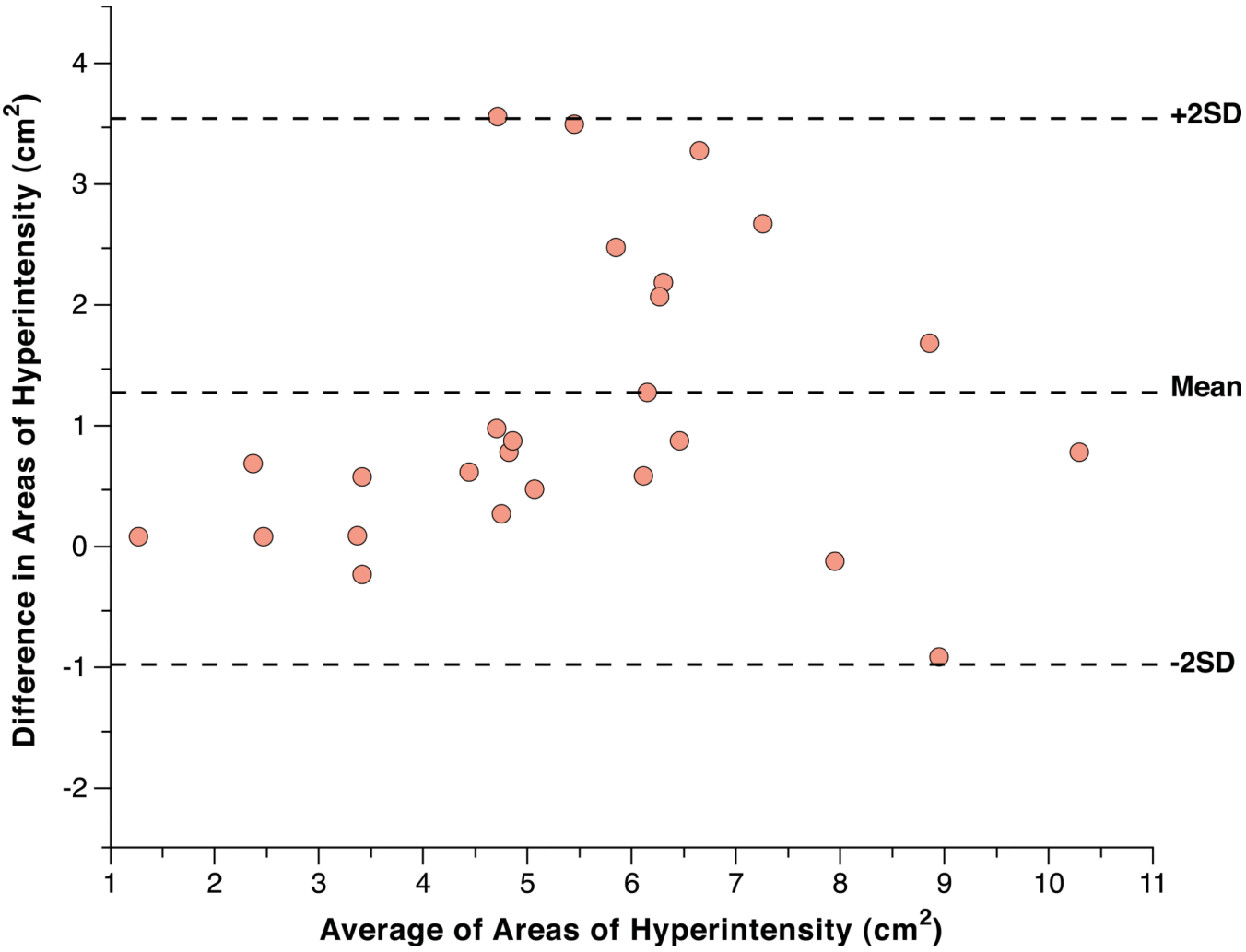

Figure 7. Bland-Altman Plot comparing the patient data for edema volume using T2-STIR and bSSFP

There was no statistically significant difference between edema volume on T2-STIR and bSSFP using a paired t-test (see Results section).